A Description of New Zealand Forest using Full-polarisation Radar Imagery

Stephen McNeill, David Pairman
Landcare Research New Zealand,
Box 69, Lincoln, New Zealand.
mcneills@landcareresearch.co.nz

Abstract

This paper describes an experiment where indices calculated from three-band full-polarisation radar imagery are regressed against key forest variables, in both exotic and indigenous forest stands. The polarimetric radar imagery is gathered in full scattering matrix form, corrected for cross-track and along-track topographic effects, after which whole-stand statistics are extracted from the imagery. Forest variables gathered vary from site to site around New Zealand, but include species, biomass, age, dbh, and stand density. The results show that the full-polarisation indices add new information over backscatter brightness regressions by giving significant correlation at high or low biomass levels. No single index provides good correlation with any single forest variable over all stand ages or biomass levels. The results suggest that a multiple-regression approach using backscatter brightness and a subset of full-polarisation indices will provide improved prediction of forest variables.

Keywords: remote sensing, radar, SAR, polarimetry

1 Introduction

When synthetic aperture radar (SAR) images a forest target, with a wavelength on the order of 3–100 cm, the backscattered response might come from the canopy, upper branches, trunk, or ground layer, depending on the wavelength, and the vegetation characteristics. For short wavelengths within the above range, the backscatter will be largely dominated by interactions at the top of the canopy layer, whereas longer wavelengths will evoke significant interaction between the top of the canopy and the base of the vegetation. Thus for a given polarisation, depending on the wavelength, the observed response from a forest layer will be the vertically integrated response from a collection of scatterers from the top of the canopy to the ground layer, and perhaps below ground.

A typical task in remote sensing is to use the integrated backscattered response, along with an appropriate model that describes the radar-forest interactions, and infer the values of parameters that describe the forest layer. Such parameters include, for example, mean values for trunk diameter, mean tree height, etc. This paper describes an experiment that uses one particular form of observed radar response (the *full-polarisation* response) and attempts to find a correlation between certain mathematical decompositions of the response and some useful forest parameters.

While it has long been recognised that there is a correlation between forest biomass (for instance) and radar backscatter brightness [1], it is also known that regressions involving these variables fail at high biomass, are species-dependent, and have poor predictive capability. The motivation of this experiment is to identify indices from full-polarisation radar data that improve the regressions between backscatter brightness and important forest variables.

Section 2 of this paper describes the characteristics of the full-polarisation radar backscatter measurement system, as well as decompositions that arise from the mathematical structure of the response. Section 3 describes the test sites and data, and the processing methodology used in the experiment. Finally, section 4 gives some preliminary results from the experiment. As results are preliminary, the final version of this paper will give a quantitative account of the observed interactions.

2 Full-polarisation SAR Imaging

2.1 The Measurement System

For an electromagnetic wave used in remote sensing, the wave state is defined by the amplitude, phase, orientation and ellipticity [2]. By making several straightforward physical assumptions [3], it is possible to show that the radar backscatter response of the target for any polarisation and ellipticity can be calculated by using the imaging arrangement in

figure 1, storing four key parameters, then applying the following synthesis procedure.

$$\sigma(\psi_r, \chi_r, \psi_t, \chi_t) = 4\pi \left| \vec{p}_r S \, \vec{p}_t \right| \quad (1)$$

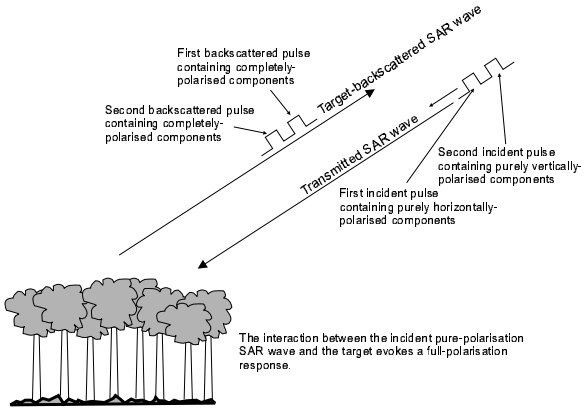

Figure 1: The full-polarisation radar imaging system

In this equation, σ is the backscatter from the target (the *radar cross section*), ψ and χ are the orientation and ellipticity respectively, the subscripts "r" and "t" refer to the "received" and "transmitted" components of ψ and χ, the vector $\vec{p}$ refers to the field polarisation vector, and S is the complex 2x2 scattering matrix. The important feature of this equation is that for each target point, one only need measure the complex 2x2 scattering matrix S to characterise the response for any given transmit-and-receive values of ellipticity and polarisation, rather than explore the whole of the backscatter-response surface. The above equation, and the process it describes, is known as *polarisation synthesis* [4].

In turns out there are alternative formulations of the polarisation synthesis equation above, using the 3x3 complex Hermitian covariance matrix C, the 4x4 symmetric real Stokes matrix M, or the 3x3 complex Hermitian coherency matrix T, which are related by way of unitary transformations [5]. The choice of which formulation one uses in a practical problem is determined by theoretical or computation convenience.

2.2 Full-polarisation Decompositions

The key characteristic of the full-polarisation imaging that is exploited in remote sensing is the inherent structure of the operator matrices (S, C, M or T) used in polarisation synthesis, and the physical relationship that this structure represents. For example, Cloude and Pottier [6] have shown that since the coherency matrix T is complex Hermitian, then its eigenvalues are real, and the corresponding eigenvectors are mutually orthogonal. The eigenvectors in this case can be physically interpreted as the parameters that define the dominant "average" scattering mechanism in the scattering element, while the eigenvalues can be interpreted as the relative strengths of these mechanisms. Thus, one might expect that a useful index would consist of some of the parameters associated with the dominant eigenvalues and eigenvectors [6].

A wide variety of decompositions or indices can be derived from the full-polarisation measurement system, using one of the operators S, C, M or T, and their number in the literature (eg described in [7]) is too numerous to describe here. In the present experiment, a selection of indices was chosen that are commonly used in the literature. The specific indices chosen are as follows (without justification, for brevity):

1. Entropy H, anisotropy A, average scattering angle $\overline{\alpha}$, defined in terms of the coherency matrix T eigenvalues [6],
2. The polarisation phase difference $\phi_{HH,VV}$ and $\phi_{HH,HV}$, and the scattering matrix correlations $\rho_{HH,VV}$ and $\rho_{HH,HV}$, between the HH and VV, and HH and HV polarisations, defined in terms of the scattering matrix S.
3. The scatterer coherence γ, defined in terms of the polarisation response from the Stokes operator M (related to the fractional polarisation in [8]).
4. Van Zyl's radar thin vegetation index RVI defined in terms of the covariance matrix C [9].
5. The equivalent number of looks ENL defined here as the ratio of the square of the mean to the variance of σ_{VV}.
6. The copolarisation and crosspolarisation differential reflectivities, ζ_{co} and ζ_{cross}, defined in terms of the polarisation response from the Stokes operator M.
7. The values of the quad-polarisation response σ_{HH}, σ_{VV} and σ_{HV} (ie. the backscatter brightness values) from the Stokes operator M.

A significant number of the indices defined in 1–7 are correlated to a greater or lesser degree. This is expected, from a theoretical analysis, and the important point is that there is a physical interpretation for the definition of the index itself.

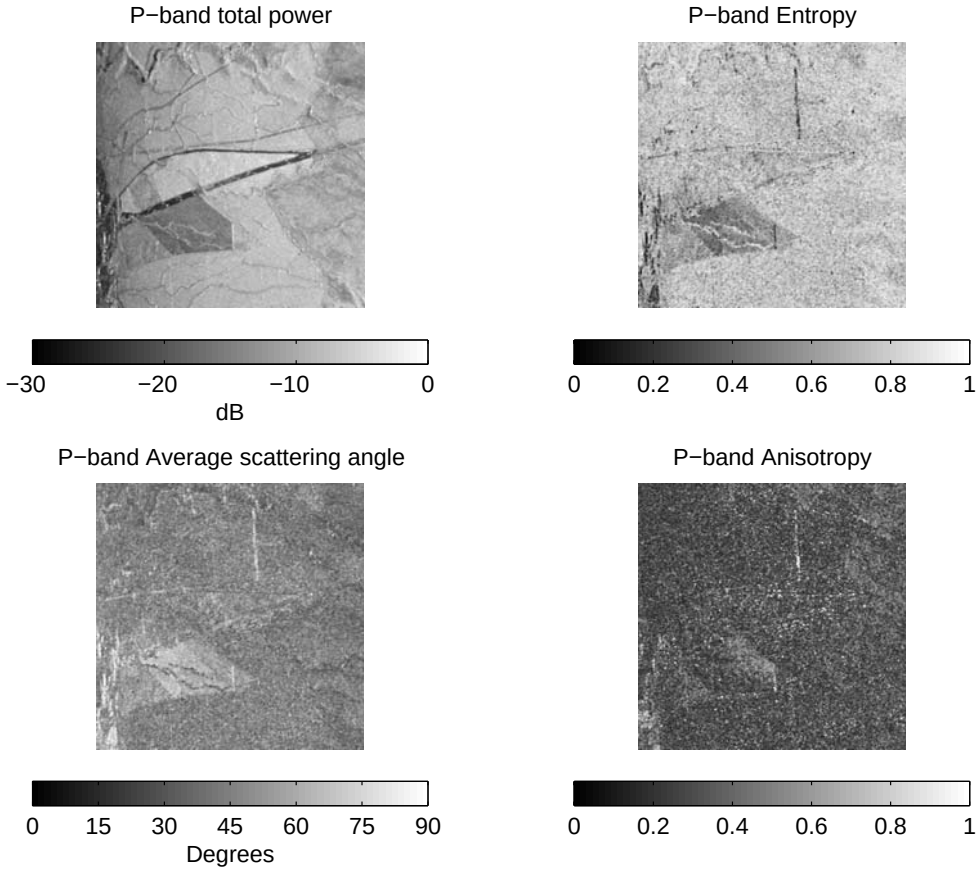

Figure 2: Sample decompositions from a P-band image (top left) total power (top right) Entropy (bottom left) Scattering angle (bottom right) Anisotropy

3 Experimental Method

3.1 Experimental Data

Imagery was gathered of New Zealand during November 1996 and August 2000, by the airborne NASA Jet Propulsion Laboratory (JPL) AIRSAR instrument [10]. In all cases, the full-polarisation Stokes Matrix operator M was available, for C-band (wavelength 5.6 cm) L-band (24 cm) and P-band (68 cm). The imagery was supplied in compressed Stokes Matrix form [11], with nominal intensity and phase calibration applied. Scenes supplied by NASA JPL were a multiple of 10 km in length, and approximately 11 km in width, with a ground resolution of 10 metres.

Imagery for this experiment was gathered over a variety of forestry sites in New Zealand, including Kaingaroa, Karioi, and Turangi in the central North Island, as well as Balmoral and the Craigieburn, Harper, Avoca catchments in the central South Island. In most cases, ground truth supporting this research was taken at the same point of time, or referred to the same time, as the imagery itself. These forestry targets cover a variety of stand ages from exotic radiata pine (Kaingaroa, Karioi, Turangi, Balmoral), Douglas fir (Kaingaroa, Turangi), and indigenous beech (Craigieburn/Harper/Avoca) and co-dominant kānuka/mānuka (Turangi). Generally, the exotic forest sites were of uniform age within a stand, whereas the indigenous sites showed some variation in regeneration state, and therefore a variety of age classes.

The available ground truth varied from site-to-site, and included some combination of: species, pruning regime, stocking density N (stems per hectare), mean stand diameter at breast height dbh, stand age y, total above-ground biomass B, mean stand height h, basal area a_B, ground slope θ_s and azimuth θ_a. A significant number of forest variables turned out to be unreliable for stands, and the most reliable variable for exotic stands turned out to be stand age. Since this variable is generally well-correlated with other stand variables, this was used as the principal aim of regression analysis.

Some parameters related to the imaging geometry were available, defining the local incidence angle and

azimuth of the surface with respect to the radar. In some cases, estimates of the variance of ground truth values were known, including a description of the probability distribution from which they were estimated.

3.2 Experimental Procedure

The three band AIRSAR data for each site was first geocoded (referenced to map coordinates) by gathering a number of ground control points (GCPs) and fitting a low-order polynomial that described the warping from the raw imagery to map coordinates, using a geometric model of the AIRSAR imaging system. The accuracy of the geocoded imagery varies from place-to-place, since it is difficult to find suitable GCPs for some regions of the country. Typical best-case rms values of 0.5 pixel and worst-case values of 1.0 pixel are achieved for areas with relatively good GCP coverage. The orthoimages were generated with a digital elevation model (DEM) generated from Land Information New Zealand (LINZ) contours with 20-metre spacing between the contours.

The Stokes Matrix operator orthoimage was then corrected for the brightness distortion due to cross-track surface slope [12] and the polarisation distortion due to along-track surface slope [13]. In general, the cross-track topographic slope correction has a significant effect, whereas the along-track topographic slope polarisation correction has only a subtle effect on the overall Stokes Matrix operator for practical targets [14]. Strictly speaking, the along-track polarisation correction need not be applied in the case of the C-band, since short wavelengths only penetrate a shorter distance into the forest layer, and are more sensitive to smaller scatterers within a resolution cell [14]. However, the correction was applied in this case, for consistency with other wavelengths.

Suitable forest stands were selected, either by imposing known Geographical Information System (GIS) forest stand boundaries on the image, or by selecting an area of a convenient size centred on a GPS-derived location from a ground plot. Where ground plots were required in exotic sites, 20-metre circular plots were used, while square plots with slope sides of 20 metres were established for indigenous sites. For Kaingaroa and Balmoral exotic forests, whole-stand forest parameters were available.

Within each selected forest stand, the average Stokes Scattering operator value $\overline{M}$ was calculated, and the corresponding average values of $\overline{S}$, $\overline{C}$ and $\overline{T}$ computed. Then, the various full-polarisation indices described in 1–7 of section 2.2 were calculated from the values of $\overline{S}$, $\overline{M}$, $\overline{C}$ or $\overline{T}$.

Linear regressions were carried out against the various polarimetric indices and the forest stand variables, applying variable or variance-stabilising transformations to correct for nonlinearity and heteroscedasticity, where these problems could be detected. The regressions were were carried out separately for each species, and the results of the regression subsequently compared. At a later stage of analysis, not discussed here, such a comparison might suggest pooling of the data from different species, in order to derive a species-invariant regression.

4 Results

It is beyond the scope of this paper to present all the detailed regressions of polarimetric indices against forest variables, since the space that would be occupied for a comprehensive description would be impractical. Instead, we present the clearest conclusions derived from the regression analysis, along with the physical interpretation of these results.

4.1 Regression analysis

In all cases, $\log(\text{Stand age})$ and log(Intensity) correlate linearly, and in the following results, log-values are always assumed. In addition, adjusted R^2 values are always quoted. The results were as follows:

- For a single-band, total power correlates with stand age, with R^2 values decreasing from P-band (66.4%) to C-band.
- A three-band total-power correlation against stand age gives an R^2 value of 73.9%, consistent with earlier findings [15]. This 3-band multiple regression is the best regression of age that can be achieved without adding polarimetric information
- Adding polarimetric information, in the form of the classical linear quad-polarisation responses, dramatically improves the correlation with stand age. The best R^2 that can be achieved with a single-band and polarisation combination is PHV (88.4%), followed by PVV (62.4%).
- If any variety of polarisations can be chosen for a single band, the best R^2 is from the three quad-polarisation components of P-band (92.2%), following by the same components of C-band (82.7%). The combination of LHH and LHV gave an R^2 of 74.7%. The apparently better performance of C-band is unexpected, and cannot be explained.
- Adding further polarisation responses does improve the regression with stand age, but it is a law of diminishing returns, since the polarisation responses become increasingly correlated. This might be expected, since the SAR response is controlled by at most nine degrees of freedom.

- Adding spatial variables to the intensity, such as the estimated number of looks (ENL), does not improve the regression with stand age. It had been expected that ENL would correlate with stand stocking, but it turned out that there was no significant relationship at all. Similarly, stand stocking has a marginally significant effect on age, but doesn't improve R^2 or the behaviour of the regression residuals.
- The entropy and scattering angle indices have a significant effect on stand age and biomass, but the correlation is highly non-linear and difficult to characterise. In particular, young exotic stands up to about 8-years old are very strongly affected by the average scattering angle, whereas older stands give very little change in either entropy or average scattering angle.
- The scatterer coherence γ correlated with above-ground biomass, but was particularly sensitive at the low-biomass scale.
- Correlation in indigenous forest was always worse than similar correlation efforts in exotic forest.
- A weak correlation was noted between cross-track local incidence angle and copolarisation phase angle, particularly for long wavelengths.

5 Discussion and Conclusions

5.1 Discussion

Conventional analysis of single-polarisation radar imagery (backscatter brightness) with forest variables generally gives significant correlations, although the nature of the correlation degrades as the uniformity of the forest stands is reduced, or if the forest is placed on significant slope. Topographic correction, applied here, reduces the degradation in these correlations.

Notably, there is a dramatic improvement in correlations with exotic stand age and indigenous stand biomass as polarimetric information is added, although care must be taken to account for collinearity in the data.

Some correlation was expected between exotic stand stocking and ENL, on the basis that ENL represents texture, and that this would alter as the stocking imcreased. In the event, there is no evidence for this correlation, although regressions with other variables are being considered.

A significant result is the strong dependence of the average scattering angle on exotic stand age and indigenous biomass. The invariance of this angle, and also entropy, at high stand ages, supports the theoretical conjecture that this index is associated with a distinct mode of scattering [5], and that it is unlikely to be useful as a general biomass index.

The key question in this study was whether the new information from polarisation radar improved multiple-regressions with stand age or biomass. The nature of the correlations between polarisation response and and forest variable suggest that significant new information is added. Notably, some forest variables and SAR variables are somewhat confusing in their relationship, especially ENL, stocking.

It is important to note that any attempt to use regression equations to derive forest variable from full-polarisation imagery assumes that any regression coefficients are universal to all types of forest. Alternatively, it assumes that there is sufficient ground truth to allow these regression relationships to be defined. It is not at all obvious that either assumption can be made, in practise, and it is a research issue whether regressions can be generated vicariously (ie. from the imagery itself) or by way of some functional model that applies to all forest types.

5.2 Conclusions

Three-band, full-polarisation imagery has been gathered for a number of exotic and indigenous forest sites across New Zealand, for which good quality ground truth is available. Indices derived from the full-polarisation imagery correlate with forest stand information with varied success. Significantly, the correlations improve as partial-polarimetric and full-polarimatric information is added. As expected, the regressions degrade in indigenous stands. Finally, there are some forest variables, such as stocking, and some radar variables, such as ENL, for which we cannot find clear relationships.

6 Acknowledgements

This work was funded by the Foundation for Research, Science and Technology. We are grateful to NASA/JPL and to their staff for bringing AIRSAR to New Zealand as part of the PACRIM missions and for their help in processing the data..

7 References

[1] Pairman, D. McNeill, S.J. Scott, N. Belliss, S. "Vegetation identification and biomass estimation using AIRSAR data", *Geocarto International*, 14(2), pp 67–75 (1999).

[2] Inan, U.S., Inan, A.S., *Engineering electromagnetics*, Addison Wesley Longman. 804 p (1999).

[3] Ulaby, F.T. van Zyl, J.J. "Wave properties and polarization". In: Ulaby, F.T. Elachi, C. (eds.) *Radar polarimetry for geoscience applications*. Norwood, Ma, Artech House. Pp. 1–16 (1990).

[4] van Zyl, J.J. Zebker, H.A. Elachi, C. “Imaging radar polarization signatures: theory and observation”. *Radio Science. 22:*529–543 (1987).

[5] Cloude, S.R. Pottier, E. “A review of target decomposition theorems in radar polarimetry”, *IEEE Transactions on Geoscience and Remote Sensing, 34:*498–518 (1996).

[6] Cloude, S.R. Pottier, E. “An entropy based classification scheme for land applications of polarimetric SAR”, *IEEE Transactions on Geoscience and Remote Sensing*, 35:68–78 (1997).

[7] Boerner, W-M. Mott, H. Lüneburg, E. *et al* “Polarimetry in radar remote sensing: basic and applied concepts”, In Henderson, F.M.; Lewis, A.J. (eds.) *Principles & applications of imaging radar*. New York, USA. J Wiley. Pp. 271–357 (1998).

[8] Zebker, H.A. van Zyl, J.J. Held, D.N. “Imaging radar polarimetry from wave synthesis”, *Journal of Geophysical Research,* 92-B1(683–701) (1987).

[9] van Zyl, J.J. “Knowledge-based land cover classification using polarimetric SAR data”, *Notes from a presentation at the PACRIM Workshop, Australasian Remote Sensing and Photogrammetry Conference*, Sydney, Australia, pp 23 (1998).

[10] Lou, Y. “Review of the NASA/JPL Airborne Synthetic Aperture Radar System”, *CD-ROM Proceedings, International Geoscience and Remote Sensing Symposium (IGARSS-02)*, Toronto, Canada, (2002).

[11] Dubois, P.C. Norikane, L. “Data volume reduction for imaging radar polarimetry”, *Proceedings of IGARSS’87*, pp 691–696 (1987).

[12] Pairman, D. Belliss, S.E. McNeill, S.J. “Terrain influences on SAR backscatter around Mt. Taranaki, New Zealand”, *IEEE Trans. Geoscience and Remote Sensing*, 35(4), pp 924–932 (1997).

[13] Lee, J-S. Schuler, D.L. Ainsworth, T.L. “Polarimetric SAR data compensation for terrain azimuth slope correction”, *IEEE Trans. Geoscience and Remote Sensing*, 38(5), pp 2153–2163 (2000).

[14] Pairman, D. McNeill,S.J. “Improved polarimetric SAR classification by application of terrain azimuth slope corrections”, *CD-ROM Proc. IGARSS’2003*, Toulouse, France (2003).

[15] Pairman, D. McNeill, S.J. “A Simulation of Radarsat-2 imagery from AIRSAR for a forestry application”, *CD-ROM Proc. Remote Sensing and Photogrammetry Association of Australasia (RSPAA)*, Adelaide, Australia (2000).

[16] Le Toan, T. Beaudoin, A. Guyon, D. “Relating forest biomass to SAR data”, *IEEE Trans. Geoscience and Remote Sensing*, 30(2), pp 403–411 (1992).